# Recipient-biased competition for a cross-fed nutrient is required for coexistence of microbial mutualists

Alexandra L. McCully, Breah LaSarre, James B. McKinlay[#]

Department of Biology, Indiana University, Bloomington, IN

Running title: Biased competition within a mutualism

[#]Corresponding author. 1001 E 3rd Street, Jordan Hall, Bloomington, IN 47405

Phone: 812-855-0359

Email: jmckinla@indiana.edu

**Conflict of interest.**

The authors declare no conflict of interest.

**Abstract.** Many mutualistic microbial relationships are based on nutrient cross-feeding. Traditionally, cross-feeding is viewed as being unidirectional from the producer to the recipient. This is likely true when a producer's metabolic waste, such as fermentation products, provides carbon for a recipient. However, in some cases the cross-fed nutrient holds value for both the producer and the recipient. In such cases, there is potential for nutrient reacquisition by producer cells in a population, leading to competition against recipients. Here we investigate the consequences of inter-partner competition for cross-fed nutrients on mutualism dynamics using an anaerobic coculture pairing fermentative *Escherichia coli* and phototrophic *Rhodopseudomonas palustris*. In this coculture, *E. coli* excretes waste organic acids that provide carbon for *R. palustris*. In return, *R. palustris* cross-feeds *E. coli* ammonium ($NH_4^+$), a valuable nitrogen compound that both species prefer. To explore the potential for inter-partner competition, we first used a kinetic model to simulate cocultures with varied affinities for $NH_4^+$ in each species. The model predicted that inter-partner competition for cross-fed $NH_4^+$ could profoundly impact population dynamics. We then experimentally tested the predictions by culturing mutants lacking $NH_4^+$ transporters in both $NH_4^+$ competition assays and cooperative cocultures. Both theoretical and experimental results indicated that the recipient must have a competitive advantage in acquiring valuable cross-fed $NH_4^+$ to avoid collapse of the mutualism. Thus, the very metabolites that form the basis for cooperative cross-feeding can also be subject to competition between mutualistic partners.

**Significance.** Mutualistic relationships, particularly those based on nutrient cross-feeding, promote stability of diverse ecosystems and drive global biogeochemical cycles. Cross-fed nutrients within these systems can be either waste products valued only by one partner or nutrients that both partners value. Here, we explore how inter-partner competition for a communally-valuable cross-fed nutrient impacts mutualism dynamics. We discovered that mutualism stability necessitates that the recipient have a competitive advantage against the producer in obtaining the cross-fed nutrient. We propose that the requirement for recipient-biased competition is a general rule for mutualistic coexistence based on the transfer of communally valuable resources, microbial or otherwise.

## Introduction

Mutualistic cross-feeding of resources between microbes can have broad impacts ranging from influencing host health (1, 2) to driving global biogeochemical cycles (3–6). Cross-fed metabolites are often regarded as nutrients due to the value they provide to a dependent partner, the recipient. However, for the partner producing the nutrient, the producer, a cross-fed nutrient's value can vary. On one extreme, the cross-fed metabolite is valued by the recipient but not the producer, as is the case for fermentative waste products (7–10). In other cases, a cross-fed metabolite holds value for both the recipient and the producer, as is the case for vitamin $B_{12}$ (6, 11, 12) and ammonium ($NH_4^+$) (13, 14). Such communally-valuable cross-fed nutrients are subject to partial privatization (15), wherein the producer has mechanisms to retain a portion of the nutrient pool for itself. While most mutualism cross-feeding studies only consider unidirectional metabolite transfer from producer to recipient, we wondered whether these mechanisms for partial privatization could lead to competition between partner populations for communally-valuable cross-fed nutrients. It seems likely that such competition could influence mutualism stability, as is known to be the case for competition for exogenous limiting resources (8, 16–19). To the best of our knowledge inter-partner competition for cross-fed nutrients and its impact on mutualism dynamics have never been investigated.

One example of cross-feeding that could involve competition between mutualistic partners is $NH_4^+$ excretion by $N_2$-fixing bacteria (Fig. 1A), called $N_2$-fixers (13, 14). During $N_2$ fixation, the enzyme nitrogenase converts $N_2$ gas into two $NH_3$ (20). In an aqueous environment, $NH_3$ is in equilibrium with $NH_4^+$. At neutral pH, $NH_4^+$ is the predominant form but small amounts of $NH_3$ can potentially leave the cell by diffusion across the membrane (21) (Fig. 1B). This inherent 'leakiness' for $NH_3$ likely fosters $NH_4^+$ cross-feeding, as extracellular $NH_3$ is available to neighboring microbes. Importantly, these neighbors can include clonal $N_2$-fixers, as $NH_3/NH_4^+$ is a preferred nitrogen source for most microbes. At concentrations above 20 μM, $NH_3$ can be acquired by passive diffusion; below 20 μM, $NH_4^+$ is bound and transported as $NH_3$ by AmtB transporters (Fig. 1B) (22). AmtB-like transporters are conserved throughout all domains of life (23). There is growing evidence that AmtB is used by $N_2$-fixers to recapture $NH_3$ lost

64 by passive diffusion, as ΔAmtB mutants accumulate $NH_4^+$ in culture supernatants whereas wild-type
65 strains do not (24–26). Thus, during $NH_4^+$ cross-feeding, AmtB likely facilitates both $NH_4^+$ acquisition by
66 the mutualistic partner and recapture of $NH_4^+$ by the $N_2$-fixer.

67 Assessing the effects of inter-partner competition for a cross-fed nutrient would require a level of
68 experimental control not possible in most natural settings. However, synthetic microbial communities, or
69 cocultures, are well-suited to address such questions (27–29). We previously developed a bacterial
70 coculture that features cross-feeding of waste products (organic acids) from *Escherichia coli*, and a
71 communally-valuable nutrient ($NH_4^+$) from *Rhodopseudomonas palustris* Nx (Fig. 1A) (26). Here, using
72 both a kinetic model and genetic manipulation to alter the affinity of each species in the coculture for
73 $NH_4^+$, we demonstrate that inter-partner competition for cross-fed $NH_4^+$ plays a direct role in maintaining
74 coexistence. Specifically, insufficient competition by *E. coli* for $NH_4^+$ resulted in a collapse of the
75 mutualism. Mutualism collapse could be delayed or potentially avoided through higher net $NH_4^+$
76 excretion by *R. palustris* or increased *E. coli* population size. Our results suggest that, as a general rule,
77 competition for a cross-fed nutrient in an obligate mutualism must be biased in favor of the recipient to
78 avoid mutualism collapse and the potential extinction of both species.
79

80 **Results**

81 **Competition for cross-fed $NH_4^+$ is predicted to shape mutualism population dynamics.** Within
82 our coculture (Fig. 1A), *E. coli* (*Ec*) ferments sugars into waste organic acids, providing essential carbon
83 and electrons to *R. palustris* (*Rp*) Nx. *R. palustris* Nx is genetically engineered to excrete low micromolar
84 amounts of $NH_4^+$, providing essential nitrogen for *E. coli* (26). $NH_4^+$ excretion by *R. palustris* Nx is due to
85 mutation of NifA, the master transcriptional regulator of nitrogenase, which results in constitutive
86 nitrogenase activity even in the presence of normally inhibitory $NH_4^+$ (30). In contrast to organic acids,
87 which are only useful to *R. palustris*, $NH_4^+$ produced by *R. palustris* Nx is essential for the growth of both
88 species; *R. palustris* uses some $NH_4^+$ for its own biosynthesis and excretes the rest, which serves as the
89 nitrogen source for *E. coli.* However, *R. palustris* Nx can also take up $NH_4^+$ (30). Thus, we hypothesized

that competition for cross-fed $NH_4^+$ between the *R. palustris* Nx producer population and the *E. coli* recipient population could influence mutualism dynamics.

We first explored whether competition for cross-fed $NH_4^+$ could affect the mutualism using SyFFoN, a mathematical model describing our coculture (26, 31). SyFFoN simulates population and metabolic dynamics in batch cocultures using Monod equations with experimentally-determined parameter values. As previous versions described $NH_4^+$ uptake kinetics only for *E. coli* (26, 31), we amended SyFFoN to include both an *R. palustris* $NH_4^+$ uptake affinity ($K_m$) and higher *R. palustris* maximum growth rate ($\mu_{MAX}$) when $NH_4^+$ is used (SI Appendix Table S1). We then simulated batch cocultures wherein the relative affinity for $NH_4^+$ varied between the two species (Fig. 2). The model predicted that coexistence is maintained when the *R. palustris* affinity for $NH_4^+$ is low relative to that of *E. coli* (*Rp*:*Ec* < 1); sufficient $N_2$ is converted to $NH_4^+$ to support *R. palustris* growth and enough $NH_4^+$ is cross-fed to support *E. coli* growth. In contrast, when the *R. palustris* affinity for $NH_4^+$ is high relative to that of *E. coli* (*Rp*:*Ec* > 1), *E. coli* growth is no longer supported because *E. coli* cannot compete for excreted $NH_4^+$. However, high *R. palustris* cell densities were still predicted (Fig. 2) due to persistent, low-level organic acid cross-feeding stemming from *E. coli* maintenance metabolism, which can support *R. palustris* growth even when *E. coli* is not growing (31).

**Genetic disruption of AmtB $NH_4^+$ transporters affects relative affinities for $NH_4^+$.** Bacterial cells generally acquire $NH_4^+$ through two mechanisms: passive diffusion of $NH_3$, or active uptake by AmtB transporters (Fig. 1B). We hypothesized that deleting *amtB* genes in either species would result in a lower affinity for $NH_4^+$ in that species and thus could be used to test how relative $NH_4^+$ affinity impacts coculture dynamics. We generated ΔAmtB mutants of both *E. coli* and *R. palustris* and first characterized the effect of the mutations in monoculture. Deletion of *amtB* in *E. coli* had no effect on growth or fermentation profiles when $NH_4Cl$ was in excess (SI Appendix Fig. S1), consistent with previous observations where ΔAmtB growth defects were only apparent at $NH_4^+$ concentrations below 20 μM (22). In *R. palustris* ΔAmtB monocultures with $N_2$ as the nitrogen source, growth trends were equivalent to

116 those of the parent strain; however, *R. palustris* ΔAmtB excreted more $NH_4^+$ than the parent strain and
117 about a third of that excreted by *R. palustris* Nx (SI Appendix Fig. S1C and D). In line with our
118 hypothesis, $NH_4^+$ excretion by *R. palustris* ΔAmtB could be due to a decreased ability to reacquire $NH_4^+$
119 lost by diffusion, resulting in increased net $NH_4^+$ excretion. Alternatively, we considered that $NH_4^+$
120 excretion by *R. palustris* ΔAmtB could be due to improper nitrogenase regulation. In several other $N_2$-
121 fixers, proper nitrogenase regulation requires AmtB, for example to induce post-translational nitrogenase
122 inhibition (switch-off) in response to $NH_4^+$ (25, 32). We tested whether *R. palustris* ΔAmtB exhibits
123 $NH_4^+$-induced switch-off by adding $NH_4Cl$ to exponentially growing cultures and measuring $H_2$
124 production, an obligate product of the nitrogenase reaction (33), as a proxy for nitrogenase activity. Upon
125 adding $NH_4Cl$, $H_2$ production stopped in *R. palustris* ΔAmtB cultures. In contrast, $H_2$ production only
126 slowed slightly in *R. palustris* Nx cultures (SI Appendix Fig. S2), consistent with previous observations
127 for NifA* strains (34, 35). Additionally, like the parent strain, *R. palustris* ΔAmtB did not produce $H_2$
128 when grown with $NH_4^+$, unlike *R. palustris* Nx (SI Appendix Fig. S3). These observations demonstrate
129 that *R. palustris* ΔAmtB is competent for $NH_4^+$-induced nitrogenase repression, and thus $NH_4^+$ excretion
130 by *R. palustris* ΔAmtB is likely due to a poor ability to reacquire $NH_4^+$ lost by diffusion.
131 To test our hypothesis that deleting *amtB* would lower cellular affinity for $NH_4^+$, we directly
132 competed all possible *E. coli* and *R. palustris* strain combinations in competition assays where ample
133 carbon was available for each species but the $NH_4^+$ concentration was kept low; specifically, a small
134 amount of $NH_4^+$ was added every hour to bring the final $NH_4^+$ concentration to 5 μM (Fig. 3). In this
135 competition assay, the species that is more competitive for $NH_4^+$ should reach a higher cell density than
136 the other species. In all cases, WT *E. coli* was more competitive for $NH_4^+$ than *R. palustris*. However,
137 each *R. palustris* strain was able to outcompete *E. coli* ΔAmtB (Fig. 3), even though the *R. palustris*
138 maximum growth rate is 4.6-times slower than that of *E. coli* (SI Appendix Fig. S1). Even *R. palustris*
139 strains lacking AmtB outcompeted *E. coli* ΔAmtB (Fig. 3), indicating that *R. palustris* has a higher
140 affinity for $NH_4^+$ than *E. coli* independent of AmtB. These data confirmed that deletion of *amtB* was an
141 effective means by which to lower the relative affinity for $NH_4^+$ in each mutualistic partner.

142 **Altering relative $NH_4^+$ affinities affects mutualistic partner frequencies.** We then examined how
143 relative affinities for $NH_4^+$ influenced mutualism dynamics by comparing the growth trends of cocultures
144 containing either WT *E. coli* or *E. coli* ΔAmtB, paired with either *R. palustris* ΔAmtB, *R. palustris* Nx, or
145 *R. palustris* NxΔAmtB, the latter of which we previously determined to exhibit 3-fold higher $NH_4^+$-
146 excretion levels than the Nx strain in monoculture (26). For each *R. palustris* partner, cocultures with *E.*
147 *coli* ΔAmtB grew slower than cocultures with WT *E. coli* (Fig. 4A,B). *E. coli* ΔAmtB also constituted a
148 lower percentage of the population and achieved lower cell densities compared to WT *E. coli* when paired
149 with the same *R. palustris* strain (Fig. 4C). These lower frequencies were consistent with the competitive
150 disadvantage of *E. coli* ΔAmtB for excreted $NH_4^+$ (Fig. 3).

151 For *R. palustris* strains lacking AmtB, the effects on population trends varied. Consistent with our
152 previous work, *R. palustris* NxΔAmtB supported higher WT *E. coli* percentages and cell densities (Fig.
153 4C) (26). With high $NH_4^+$ excretion levels from *R. palustris* NxΔAmtB, faster *E. coli* growth leads to
154 rapid organic acid accumulation, which acidifies the environment, inhibits *R. palustris* growth, and leaves
155 organic acids unconsumed (Fig. 4D) (26). Surprisingly, although *R. palustris* ΔAmtB excreted less $NH_4^+$
156 than *R. palustris* Nx in monoculture, *R. palustris* ΔAmtB supported a higher WT *E. coli* population in
157 coculture and consumable organic acids accumulated (Fig. 4C, D). These trends resemble those from
158 cocultures with *R. palustris* NxΔAmtB (Fig. 4C, D), which has a high level of $NH_4^+$ excretion (SI
159 Appendix Fig. S1D). Unlike Nx strains, which have constitutive nitrogenase activity due to a mutation in
160 the transcriptional activator NifA (30), *R. palustris* ΔAmtB has WT NifA. Thus, *R. palustris* ΔAmtB can
161 likely still regulate nitrogenase expression, and thereby its activity, in response to nitrogen starvation. We
162 hypothesized that in coculture with WT *E. coli*, *R. palustris* ΔAmtB might experience heightened
163 nitrogen starvation, as $NH_4^+$ consumption by WT *E. coli* would limit $NH_4^+$ reacquisition by *R. palustris*
164 ΔAmtB (in an *R. palustris* ΔAmtB monoculture any lost $NH_4^+$ would remain available to *R. palustris*).
165 We therefore tested whether coculture conditions stimulated higher nitrogenase activity using an
166 acetylene reduction assay. In agreement with our hypothesis, *R. palustris* ΔAmtB had increased
167 nitrogenase activity in coculture conditions compared to monocultures, whereas *R. palustris* Nx, which

168 exhibits constitutive nitrogenase activity, showed similar levels in both conditions (SI Appendix Fig. S4).
169 Thus, the relatively high WT *E. coli* population in coculture with *R. palustris* ΔAmtB is likely due to both
170 the competitive advantage for acquiring $NH_4^+$ over *R. palustris* ΔAmtB (Fig. 3) and higher $NH_4^+$ cross-
171 feeding levels due to increased nitrogenase activity.
172
173 ***E. coli* must have a competitive advantage for $NH_4^+$ acquisition to avoid mutualism collapse.** We
174 were surprised to observe that cocultures of *R. palustris* ΔAmtB paired with *E. coli* ΔAmtB showed little
175 growth when started from a single colony of each species (Fig. 4A), a method that we routinely use to
176 initiate cocultures (26, 31). We reasoned that the higher *R. palustris* ΔAmtB affinity for $NH_4^+$ relative to
177 *E. coli* ΔAmtB (Fig. 3) likely led to community collapse as predicted by SyFFoN (Fig. 2). Even though
178 SyFFoN had predicted *R. palustris* growth when outcompeting *E. coli* for $NH_4^+$ (Fig. 2), SyFFoN likely
179 underestimates the time required to achieve these densities, if they would be achieved at all, as SyFFoN
180 does not take into account cell death, which is known to occur when *E. coli* growth is prevented (31).
181 Consistent with the hypothesis that poor coculture growth was due to a competitive disadvantage of *E.*
182 *coli* ΔAmtB for $NH_4^+$, SyFFoN simulations indicated that starting with a larger *E. coli* ΔAmtB population
183 would increase the probability that any given *E. coli* cell would acquire $NH_4^+$ versus *R. palustris* and
184 thereby overcome the competitive disadvantage of *E. coli* ΔAmtB for $NH_4^+$ (SI Appendix Fig. S5).
185 Indeed, we observed greater growth of both species when cocultures were inoculated with equal or higher
186 relative densities of *E. coli* ΔAmtB versus *R. palustris* ΔAmtB (SI Appendix Fig. S5).
187 The explanation that mutualism collapse was due to a competitive advantage of *R. palustris* ΔAmtB
188 over *E. coli* ΔAmtB for $NH_4^+$ called into question why cocultures pairing *E. coli* ΔAmtB with either *R.*
189 *palustris* Nx or *R. palustris* NxΔAmtB did not collapse as well (Fig. 4), given that in all of these pairings
190 *E. coli* ΔAmtB is at competitive disadvantage (Fig. 3). We hypothesized that a relatively high $NH_4^+$
191 excretion level by these latter *R. palustris* strains (SI Appendix Fig. S1D) could compensate for a low *E.*
192 *coli* $NH_4^+$ affinity. To explore this hypothesis we simulated cocultures with the *R. palustris* affinity for
193 $NH_4^+$ set high relative to that of *E. coli* (*Rp*:*Ec* = 1000) and varied the *R. palustris* $NH_4^+$ excretion level

194 (Fig. 5). Indeed, increasing *R. palustris* $NH_4^+$ excretion was predicted to overcome a low *E. coli* affinity
195 for $NH_4^+$ and support growth of both species (Fig. 5). The only exception was at the highest levels of
196 $NH_4^+$ excretion, where *R. palustris* growth was predicted to be inhibited due to rapid *E. coli* growth and
197 subsequent accumulation of organic acids that acidify the environment (Fig. 5) (26). These simulations
198 suggested that *R. palustris* Nx and NxΔAmtB supported coculture growth with *E. coli* ΔAmtB due to
199 higher $NH_4^+$ excretion levels (SI Appendix Fig. S1D), whereas a combination of low $NH_4^+$ excretion by
200 *R. palustris* ΔAmtB (SI Appendix Fig. S1D) and a low affinity for $NH_4^+$ by *E. coli* ΔAmtB led to collapse
201 of the mutualism in this pairing.

202 So far, we had only considered the effect of severe discrepancies in $NH_4^+$ affinities between the two
203 species (e.g., 1000-fold difference in $K_m$ values in our simulations) as a mechanism leading to coculture
204 collapse within the time period of a single culturing. However, we wondered if a subtle discrepancy in
205 $NH_4^+$ affinities could lead to coculture collapse if given more time. We therefore simulated serial transfers
206 of cocultures with partners having different relative $NH_4^+$ affinities (Fig. 6A, B). At equivalent $NH_4^+$
207 affinities (Fig. 6A), both species were predicted to be maintained over serial transfers. However, when the
208 relative affinities approached a threshold (relative *Rp*:*Ec* = 2.75), cell densities of both species were
209 predicted to decrease over serial transfers (Fig. 6B). This decline in coculture growth is due to *E. coli*
210 being slowly but progressively outcompeted for $NH_4^+$ by *R. palustris*. As the difference between the *R.*
211 *palustris* and *E. coli* populations expands, *R. palustris* cells have a greater chance of acquiring $NH_4^+$ than
212 the smaller *E. coli* population, further starving *E. coli* and simultaneously cutting off *R. palustris* from its
213 supply of organic acids from *E. coli.*

214 The above prediction prompted us to investigate if cocultures pairing *R. palustris* Nx with *E. coli*
215 ΔAmtB were stable through serial transfers. We focused on cocultures with *R. palustris* Nx rather than *R.*
216 *palustris* NxΔAmtB because *R. palustris* Nx has AmtB and would therefore be most likely to outcompete
217 *E. coli* ΔAmtB. Strikingly, after eight serial transfers of cocultures pairing *R. palustris* Nx with *E. coli*
218 ΔAmtB we observed coculture collapse (Fig. 6C). This observation is in stark contrast to cocultures of *R.*
219 *palustris* Nx paired with WT *E. coli*, which we have serially transferred for over 100 times with no

extinction events (unpublished data). These results indicate that the recipient population must have a competitive advantage for a cross-fed nutrient versus the producer population to avoid mutualism collapse.

**Discussion**

Here we demonstrate that mutualistic partners can compete for a cross-fed nutrient upon which the mutualistic interaction is based, in this case $NH_4^+$. This competition can impact partner frequencies and mutualism stability. Efficient nutrient reacquisition by the producer can render nutrient excretion levels insufficient for cooperative growth, starving the recipient and leading to tragedy of the commons (36). Conversely, recipient-biased competition for a cross-fed nutrient drives cooperative directionality in nutrient exchange and thereby promotes mutualism stability. One implication of these results is that inter-partner competition can influence the level of resource privatization. Within microbial interdependencies, partial privatization has primarily been thought to depend on mechanisms used by the producer to retain a portion of a communally-valuable resource (15). Our data indicate that for excreted resources having a transient availability to both mutualists, recipient acquisition mechanisms can also influence the level of producer privatization, as the competition impacts how much of a cross-fed resource will be shared versus re-acquired. In effect, recipient-biased competition avoids tragedy of the commons by enforcing partial privatization of a communally-valuable resource. The importance of the recipient having the upper hand in inter-partner competition likely applies to other synthetic cocultures and natural microbial mutualisms that are based on the cross-feeding of communally-valuable nutrients, including amino acids (37, 38) and vitamin $B_{12}$ (6, 11). The same rule could also apply to inter-kingdom and non-microbial examples of cross-feeding (e.g., plants and pollinators, nutrient transfer between plants and bacteria or fungi (39)) and cooperative feeding (e.g., honeyguide bird and human harvesting of bee hives (40), cooperative hunting between grouper fish and moray eels (41)). In such cases, increased privatization of a cross-fed or shared resource, for example through producer-biased competition, could threaten the mutualism upon which both species depend (15, 39, 42).

246 In our system, AmtB transporters were crucial determinants of inter-partner competition for $NH_4^+$.
247 We were intrigued to find that when both species lacked AmtB, *R. palustris* out-competed *E. coli* for
248 $NH_4^+$ (Fig. 5), enough so to collapse the mutualism within a single culturing (Fig. 3). Whether by
249 maximizing $NH_4^+$ retention or re-acquisition, *R. palustris*, and perhaps other $N_2$-fixers, might have
250 additional mechanisms aside from AmtB to minimize loss of $NH_4^+$ as $NH_3$. These mechanisms could
251 include a relatively low internal pH to favor $NH_4^+$ over $NH_3$, negatively-charged surface features, or
252 relatively high affinities by $NH_4^+$-assimilating enzymes such as glutamine synthetase. There are several
253 reasons why it would be beneficial for $N_2$-fixers to minimize $NH_4^+$ loss. First, $N_2$ fixation is expensive,
254 both in terms of the enzymes involved (43) and the reaction itself, costing 16 ATP to convert one $N_2$ into
255 two $NH_3$ (33). Passive loss of $NH_3$ would only add to this cost, as more $N_2$ would have to be fixed to
256 compensate. Second, loss of $NH_4^+$ could benefit nearby microbes competing against an $N_2$-fixer for
257 separate limiting nutrients (14, 44). The possibility that $N_2$-fixers could have a superior ability to retain or
258 acquire $NH_4^+$ independently of AmtB is not farfetched. Bacteria are known to exhibit differential abilities
259 to compete for nutrients. For example, iron acquisition commonly involves iron-binding siderophores, but
260 siderophores can be chemically distinct and thereby differ in their affinity for iron (45). Strategies to
261 utilize siderophores as a shared resource are also numerous, leading to different cooperative or
262 competitive outcomes in microbial communities (45, 46). One must consider that additional mechanisms
263 for acquiring $NH_4^+$ beyond AmtB might likewise exist. As our results have raised the potential for inter-
264 partner competition for cross-fed resources themselves, understanding the physiological mechanisms that
265 confer competitive advantages for nutrient acquisition between species will undoubtedly aid in describing
266 the interplay between competition and cooperation within mutualisms.
267

268 **Materials and Methods**

269 **Strains and growth conditions.** Strains, plasmids, and primers are listed in SI Appendix Table S2. All *R.*
270 *palustris* strains contained *ΔuppE* and *ΔhupS* mutations to facilitate accurate colony forming unit (CFU)
271 measurements by preventing cell aggregation (47) and to prevent $H_2$ uptake, respectively. *E. coli* was

272 cultivated on Luria-Burtani (LB) agar and *R. palustris* on defined mineral (PM) (48) agar with 10 mM
273 succinate. $(NH_4)_2SO_4$ was omitted from PM agar for determining *R. palustris* CFUs. Monocultures and
274 cocultures were grown in 10-mL of defined M9-derived coculture medium (MDC) (26) in 27-mL
275 anaerobic test tubes. To make the medium anaerobic, MDC was bubbled with $N_2$, then tubes were sealed
276 with rubber stoppers and aluminum crimps, and then autoclaved. After autoclaving, MDC was
277 supplemented with cation solution (1 % v/v; 100 mM $MgSO_4$ and 10 mM $CaCl_2$) and glucose (25 mM),
278 unless indicated otherwise. *E. coli* monocultures were also supplemented with 15mM $NH_4Cl$. All cultures
279 were grown at 30°C laying horizontally under a 60 W incandescent bulb with shaking at 150 rpm. Starter
280 cocultures were inoculated with 200 µL MDC containing a suspension of a single colony of each species.
281 Test cocultures were inoculated using a 1% inoculum from starter cocultures. Serial transfers were also
282 inoculated with a 1% inoculum. Kanamycin and gentamycin were added to a final concentration of 100
283 µg/ml for *R. palustris* and 15 µg/ml for *E. coli* where appropriate.
284 **Generation of *R. palustris* mutants.** *R. palustris* mutants were derived from wild-type CGA009 (49).
285 Generation of strains CGA4004, CGA4005, and CGA4021 was described previously (26). For generation
286 of strain CGA4026 (*R. palustris* ΔAmtB) the WT *nifA* gene was amplified using primers JBM1 and
287 JBM2, digested with XbaI and BamHI, and ligated into plasmid pJQ200SK to make pJQnifA16. This
288 suicide vector was then introduced into CGA4021 by conjugation, and sequential selection and screening
289 was performed as described (50) to replace *nifA** with WT *nifA*. Reintroduction of the WT *nifA* gene was
290 confirmed by PCR and sequencing.
291 **Generation of the *E. coli* ΔAmtB mutant.** P1 transduction (51) was used to introduce Δ*amtB::Km* from
292 the Keio collection strain JW0441-1 (52) into MG1655. The Δ*amtB::Km* genotype of kanamycin-resistant
293 colonies was confirmed by PCR and sequencing.
294 **Analytical procedures.** Cell density was assayed by optical density at 660 nm ($OD_{660}$) using a Genesys
295 20 visible spectrophotometer (Thermo-Fisher, Waltham, MA, USA). Growth curve readings were taken
296 in culture tubes without sampling (i.e., Tube $OD_{660}$). Specific growth rates were determined using
297 readings between 0.1-1.0 $OD_{660}$ where there is linear correlation between cell density and $OD_{660}$. Final

298 $OD_{660}$ measurements were taken in cuvettes and samples were diluted into the linear range as necessary.
299 $H_2$ was quantified using a Shimadzu (Kyoto, Japan) gas chromatograph (GC) with a thermal conductivity
300 detector as described (53). Glucose, organic acids, formate and ethanol were quantified using a Shimadzu
301 high-performance liquid chromatograph (HPLC) as described (54). $NH_4^+$ was quantified using an
302 indophenol colorimetric assay as described (26).
303 **Nitrogenase activity.** Nitrogenase activity was measured using an acetylene reduction assay (43). Cells
304 from 10-mL cultures were harvested and resuspended in 10-mL fresh MDC medium in 27-mL sealed
305 tubes pre-flushed with argon gas. Suspensions were incubated in light for 1 h at 30°C to recover. Then,
306 250 µl of 100% acetylene gas was injected into the headspace to initiate the assay, and ethylene
307 production was measured over time by gas chromatography as described (43). Ethylene levels were
308 normalized to total *R. palustris* CFUs in the 10-ml volume.
309 **$NH_4^+$ competition assay.** Fed-batch cultures were performed in custom anaerobic 75-ml serum vials with
310 side sampling ports. Each vial contained a stir bar and 30-mL of MDC, and was sealed at both ends with
311 rubber stoppers and aluminum crimps. Each vial was supplemented with 25 mM glucose, 1 % v/v cation
312 solution and 20 mM sodium acetate. Starter monocultures of each species were grown to equivalent
313 CFUs/mL in MDC tubes containing limiting nutrients (3 mM sodium acetate for *R. palustris* and 1.5 mM
314 $NH_4Cl$ for *E. coli*), and 1 mL of each species was inoculated into the serum vials. These competition
315 cocultures were incubated at 30°C under a 60 W incandescent bulb with stirring at 200 rpm (Thermo
316 Scientific) for 96 h. Each serum vial was constantly flushed with Ar to maintain anaerobic conditions.
317 $NH_4Cl$ was fed from a 500 µM $NH_4Cl$ stock using a peristaltic pump (Watson-Marlow) on an automatic
318 timer (Intermatic DT620) at a rate of 0.33 mL/min once an hour for a final concentration of ~ 5 µM upon
319 each addition. Samples were taken at 0 and 96 h for quantification of CFUs.
320 **Mathematical modeling.** A Monod model describing bi-directional cross-feeding in batch cultures,
321 called SyFFoN_v3 (Syntrophy between Fermenter and Fixer of Nitrogen), was modified from our
322 previous model (31) to allow for competition between *E. coli* and *R. palustris* for $NH_4^+$ as follows: (i) an
323 equation for *R. palustris* growth rate on $NH_4^+$ was added to boost the *R. palustris* growth rate when

acquiring $NH_4^+$ and (ii) the ability for *R. palustris* to consume $NH_4^+$ was added along with a $K_m$ of *R. palustris* for $NH_4^+$ ($K_{AR}$). Equations and default parameter values are in the SI Appendix and Table S1. SyFFoN_v3 runs in R studio and is available for download at: https://github.com/McKinlab/Coculture-Mutualism.

**Acknowledgments**

We thank Richard Phillips (Indiana University) for providing equipment for the $NH_4^+$ competition assay. We also thank Jay Lennon (Indiana University) for helpful discussions on the manuscript. This work was supported in part by the U.S. Department of Energy, Office of Science, Office of Biological and Environmental Research, under Award Number DE-SC0008131, by the U.S. Army Research Office, grant W911NF-14-1-0411, and by the Indiana University College of Arts and Sciences.

**References**

1. Flint HJ, Duncan SH, Scott KP, Louis P. (2007) Interactions and competition within the microbial community of the human colon: Links between diet and health. *Environ Microbiol.* **9**(5):1101–1111.
2. Hammer ND, et al. (2014) Inter- and intraspecies metabolite exchange promotes virulence of antibiotic-resistant *Staphylococcus aureus*. *Cell Host Microbe.* **16**(4):531–537.
3. McInerney MJ, Sieber JR, Gunsalus RP. (2010) Syntrophy in anaerobic global carbon cycles. *Curr Opin Biotechnol.* **20**(6):623–632.
4. Durham BP, et al. (2015) Cryptic carbon and sulfur cycling between surface ocean plankton. *Proc Natl Acad Sci U S A.* **112**(2):453–457.
5. Reeburgh WS. (2007) Oceanic Methane Biogeochemistry. *Chem Rev.* **107**(2):486–513.
6. Croft MT, Lawrence AD, Raux-Deery E, Warren MJ, Smith AG. (2005) Algae acquire vitamin $B_{12}$ through a symbiotic relationship with bacteria. *Nature.* **438**:90–93.
7. McInerney MJ, et al. (2008) Physiology, ecology, phylogeny, and genomics of microorganisms capable of syntrophic metabolism. *Ann N Y Acad Sci.* **1125**:58–72.

8. Hillesland KL, Stahl DA. (2010) Rapid evolution of stability and productivity at the origin of a microbial mutualism. *Proc Natl Acad Sci U S A.* **107**(5):2124–2129.
9. Schink B. (1997) Energetics of syntrophic cooperation in methanogenic degradation. *Microbiol Mol Biol Rev.* **61**(2):262–280.
10. Stams AJM. (1994) Metabolic interactions between anaerobic bacteria in methanogenic environments. *Antonie van Leeuwenhoek, Int J Gen Mol Microbiol.* **66**:271–294.
11. Grant MA, Kazamia E, Cicuta P, Smith AG. (2014) Direct exchange of vitamin $B_{12}$ is demonstrated by modeling the growth dynamics of algal-bacterial cocultures. *ISME J* **8**(7):1–10.
12. Seth EC, Taga ME. (2014) Nutrient cross-feeding in the microbial world. *Front Microbiol.* **5**:1-6.
13. Behrens S, et al. (2008) Linking microbial phylogeny to metabolic activity at the single-cell level by using enhanced element labeling-catalyzed reporter deposition fluorescence in situ hybridization (EL-FISH) and NanoSIMS. *Appl Environ Microbiol.* **74**(10):3143–3150.
14. Adam B et al. (2016) $N_2$-fixation, ammonium release and N-transfer to the microbial and classical food web within a plankton community. *ISME J.* **10**:450-459.
15. Estrela S, Morris JJ, Kerr B (2016) Private benefits and metabolic conflicts shape the emergence of microbial interdependencies. *Environ Microbiol.* **18**(5):1415–1427.
16. Meyer JS, Tsuchiya HM. (1975) Dynamics of mixed populations having complementary metabolism. *Biotechnol Bioeng.* **17**:1065–1081.
17. Kim HJ, Boedicker JQ, Choi JW, Ismagilov RF. (2008) Defined spatial structure stabilizes a synthetic multispecies bacterial community. *Proc Natl Acad Sci U S A.* **105**(47):18188–18193.
18. Miura Y, Tanaka H, Okazaki M. (1980) Stability analysis of commensal and mutual relations with competitive assimilation in continuous mixed culture. *Biotechnol Bioeng.* **22**(5):929–946.
19. Estrela S, Trisos CH, Brown SP. (2012) From metabolism to ecology: cross-feeding interactions shape the balance between polymicrobial conflict and mutualism. *Am Nat.* **180**(5):566–576.
20. Bulen WA, LeComte JR. (1966) The nitrogenase system from *Azotobacter*: two-enzyme requirement for $N_2$ reduction, ATP-dependent $H_2$ evolution, and ATP hydrolysis. *Proc Natl Acad Sci U S A.* **56**(3):979–986.

377 21. Walter A, Gutknecht J. (1986) Permeability of small nonelectrolytes through lipid bilayer membranes. *J*
378 *Membr Biol.* **90**(3):207–217.
379 22. Kim M, et al. (2012) Need-based activation of ammonium uptake in *Escherichia coli*. *Mol Syst Biol*
380 **8**(616):1–10.
381 23. Peng J, Huang CH. (2006) Rh proteins vs Amt proteins: an organismal and phylogenetic perspective on
382 $CO_2$ and $NH_3$ gas channels. *Transfus Clin Biol.* **13**(1–2):85–94.
383 24. Barney BM, Eberhart LJ, Ohlert JM, Knutson CM, Plunkett MH. (2015) Gene deletions resulting in
384 increased nitrogen release by *Azotobacter vinelandii*: Application of a novel nitrogen biosensor. *Appl*
385 *Environ Microbiol.* **81**(13):4316–4328.
386 25. Zhang T, et al. (2012) Involvement of the ammonium transporter AmtB in nitrogenase regulation and
387 ammonium excretion in *Pseudomonas stutzeri* A1501. *Res Microbiol.* **163**(5):332–339.
388 26. LaSarre B, McCully AL, Lennon JT, McKinlay JB. (2017) Microbial mutualism dynamics governed by
389 dose-dependent toxicity of cross-fed nutrients. *ISME J.* **11**:337–348.
390 27. Widder S, et al. (2016) Challenges in microbial ecology: building predictive understanding of community
391 function and dynamics. *ISME J.* **10**:2557–2568.
392 28. Momeni B, Chen CC, Hillesland KL, Waite A, Shou W. (2011) Using artificial systems to explore the
393 ecology and evolution of symbioses. *Cell Mol Life Sci.* **68**(8):1353–1368.
394 29. Lindemann SR, et al. (2016) Engineering microbial consortia for controllable outputs. *ISME J.* **10**:2077–
395 2084.
396 30. McKinlay JB, Harwood CS. (2010) Carbon dioxide fixation as a central redox cofactor recycling
397 mechanism in bacteria. *Proc Natl Acad Sci U S A.* **107**(26):11669–11675.
398 31. McCully AL, LaSarre B, McKinlay JB. (2017) Growth-independent cross-feeding modifies boundaries for
399 coexistence in a bacterial mutualism. *biorXiv*. **doi:** https://doi.org/10.1101/083386
400 32. Yakunin AF, Hallenbeck PC. (2002) AmtB is necessary for $NH_4^+$-induced nitrogenase switch-off and
401 ADP-ribosylation in *Rhodobacter capsulatus*. *J Bacteriol.* **184**(15):4081–4088.
402 33. Hoffman BM, Lukoyanov D, Dean DR, Seefeldt LC. (2013) Nitrogenase: A draft mechanism. *Acc Chem*
403 *Res.* **46**(2):587–595.

404 34. Rey FE, Heiniger EK, Harwood CS. (2007) Redirection of metabolism for biological hydrogen
405 production. *Appl Environ Microbiol.* **73**(5):1665–1671.
406 35. Heiniger EK, Oda Y, Samanta SK, Harwood CS. (2012) How posttranslational modification of
407 nitrogenase is circumvented in *Rhodopseudomonas palustris* strains that produce hydrogen gas
408 constitutively. *Appl Environ Microbiol.* **78**(4):1023–1032.
409 36. Rankin DJ, Bargum K, Kokko H. (2007) The tragedy of the commons in evolutionary biology. *Trends*
410 *Ecol Evol.* **22**(12):643–651.
411 37. Pande S, et al. (2014) Fitness and stability of obligate cross-feeding interactions that emerge upon gene
412 loss in bacteria. *ISME J.* **8**(5):953–62.
413 38. Harcombe W. (2010) Novel cooperation experimentally evolved between species. *Evolution.* **64**(7):2166–
414 2172.
415 39. Bronstein JL. (2001) The Exploitation of Mutualisms. *Ecol Lett.* **4**:277–287.
416 40. Isack HA, Reyer H-U. (1989) Honeyguides and honey gatherers: Interspecific communication in a
417 symbiotic relationship. *Science.* **243**(4896):1343–1346.
418 41. Bshary R, Hohner A, Ait-el-Djoudi K, Fricke H. (2006) Interspecific communicative and coordinated
419 hunting between groupers and giant moray eels in the red sea. *PLoS Biol* **4**(12):2393–2398.
420 42. Sachs JL, Mueller UG, Wilcox TP, Bull JJ. (2004) The evolution of cooperation. *Q Rev Biol.* **51**(2):211–
421 244.
422 43. Oda Y, et al. (2005) Functional genomic analysis of three nitrogenase isozymes in the photosynthetic
423 bacterium *Rhodopseudomonas palustris*. *Am Soc Microbiol.* 187(22):7784–7794.
424 44. Morris JJ, Lenski RE, Zinser ER. (2012) The black queen hypothesis: Evolution of dependencies through
425 adaptive gene loss. *mBio.* **3**(2):1–7.
426 45. Joshi F, Archana G, Desai A. (2006) Siderophore cross-utilization amongst rhizospheric bacteria and the
427 role of their differential affinities for $Fe^{3+}$ on growth stimulation under iron-limited conditions. *Curr*
428 *Microbiol.* **53**(2):141–147.
429 46. Niehus R, Picot A, Oliveira NM, Mitri S, Foster KR. (2017) The evolution of siderophore production as a
430 competitive trait. *Evolution*. doi:10.1111/evo.13230.

431 47. Fritts RK, Lasarre B, Stoner AM, Posto AL, Mckinlay JB (2017) A *Rhizobiales*-specific unipolar
432 polysaccharide adhesin contributes to *Rhodopseudomonas palustris* biofilm formation across diverse
433 photoheterotrophic conditions. *Appl Environ Microbiol.* **83**(4):1–14.
434 48. Kim M-K, Harwood CS (1991) Regulation of benzoate-CoA ligase in *Rhodopseudomonas palustris*.
435 *FEMS Microbiol Lett.* **83**:199–203.
436 49. Larimer FW, et al. (2004) Complete genome sequence of the metabolically versatile photosynthetic
437 bacterium *Rhodopseudomonas palustris*. *Nat Biotechnol.* **22**(1):55–61.
438 50. Rey FE, Oda Y, Harwood CS. (2006) Regulation of uptake hydrogenase and effects of hydrogen
439 utilization on gene expression in *Rhodopseudomonas palustris*. *J Bacteriol.* **188**(17):6143–6152.
440 51. Thomason LC, Costantino N, Court DL. (2007) *E. coli* Genome manipulation by P1 transduction. *Curr*
441 *Protoc Mol Biol.* doi 10.1002/0471142727.mb0117s79
442 52. Baba T, et al. (2006) Construction of *Escherichia coli* K-12 in-frame, single-gene knockout mutants: the
443 Keio collection. *Mol Syst Biol.* **2**:2006.0008.
444 53. Huang JJ, Heiniger EK, McKinlay JB, Harwood CS. (2010) Production of hydrogen gas from light and the
445 inorganic electron donor thiosulfate by *Rhodopseudomonas palustris*. *Appl Environ Microbiol.*
446 **76**(23):7717–7722.
447 54. McKinlay JB, Zeikus JG, Vieille C. (2005) Insights into *Actinobacillus succinogenes* fermentative
448 metabolism in a chemically defined growth medium. *Appl Env Microbiol.* **71**(11):6651–6656.
449

450 **Figure Legends**

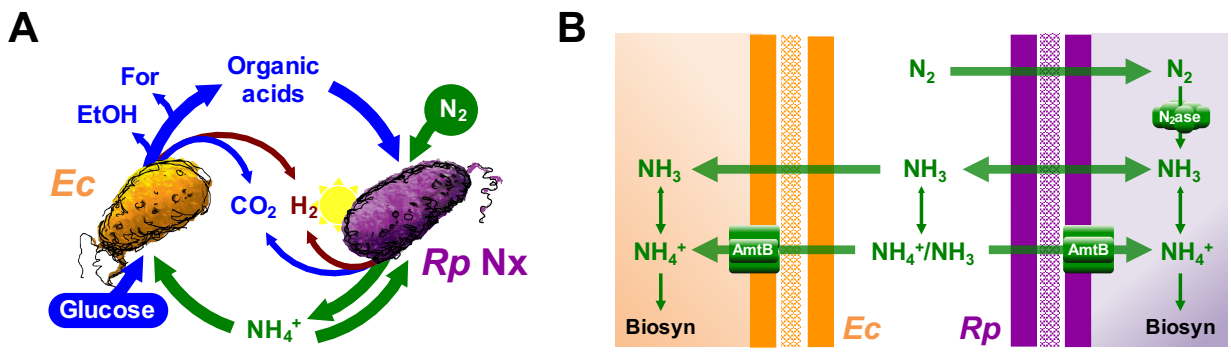


451

452 **Fig. 1. Mechanisms of $NH_4^+$ transfer within an obligate bacterial mutualism based on cross-feeding**
453 **of essential nutrients.** (**A**) *Escherichia coli* (*Ec*) anaerobically ferments glucose into organic acids,
454 supplying *Rhodopseudomonas palustris* Nx (*Rp* Nx) with essential carbon. *R. palustris* Nx fixes $N_2$ gas
455 and excretes $NH_4^+$, supplying *E. coli* with essential nitrogen. For, formate; EtOH, ethanol. (**B**) $NH_4^+$ can
456 be passively lost from cells as $NH_3$. Both species encode high-affinity $NH_4^+$ transporters, AmtB, that
457 facilitate $NH_4^+$ uptake. $NH_4^+$ is the predominant form at neutral pH, as indicated by an enlarged arrow
458 head on double-sided arrows.

459

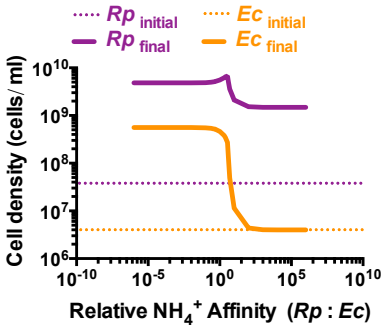


460

461 **Fig. 2. Simulations suggest that *E. coli* must have a competitive advantage for $NH_4^+$ acquisition**
462 **relative to *R. palustris* to support mutualistic growth**. Final cell densities (solid lines) of *R. palustris*
463 (*Rp*, purple) and *E. coli* (*Ec*, orange) after 300 h in simulated batch cultures for a range of relative $NH_4^+$
464 affinities. Initial cell densities are indicated by dotted lines. Relative $NH_4^+$ affinity values represent the
465 relative *E. coli* $K_m$ for $NH_4^+$ ($K_A$) divided by that of *R. palustris* ($K_{AR}$).

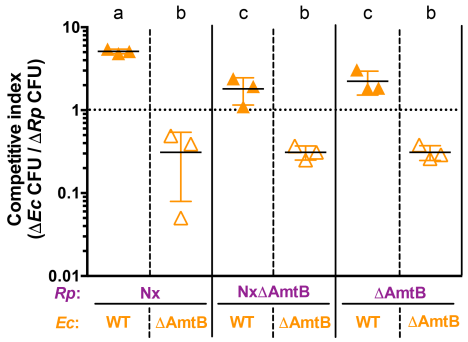


**Fig. 3. AmtB is important for competitive $NH_4^+$ acquisition.** Competitive indices for *E. coli* after 96 h in $NH_4^+$-limited competition assay cocultures. Cocultures were inoculated with *E. coli* and *R. palustris* at equivalent cell densities with excess carbon available for both species (25 mM glucose for *E. coli* and 20 mM sodium acetate for *R. palustris*). $NH_4^+$ was added to cocultures to a final concentration of 0.5 µM every hour for 96 h. The dotted line indicates a competitive index value of 1, where both species are equally competitive for $NH_4^+$. Filled triangles, WT *E. coli*; open triangles *E. coli* ΔAmtB. Error bars indicate SD, n=3. Different letters indicate statistical differences between *E. coli* competitive index values, $p < 0.05$, determined by one-way ANOVA with Tukey's multiple comparisons post test.

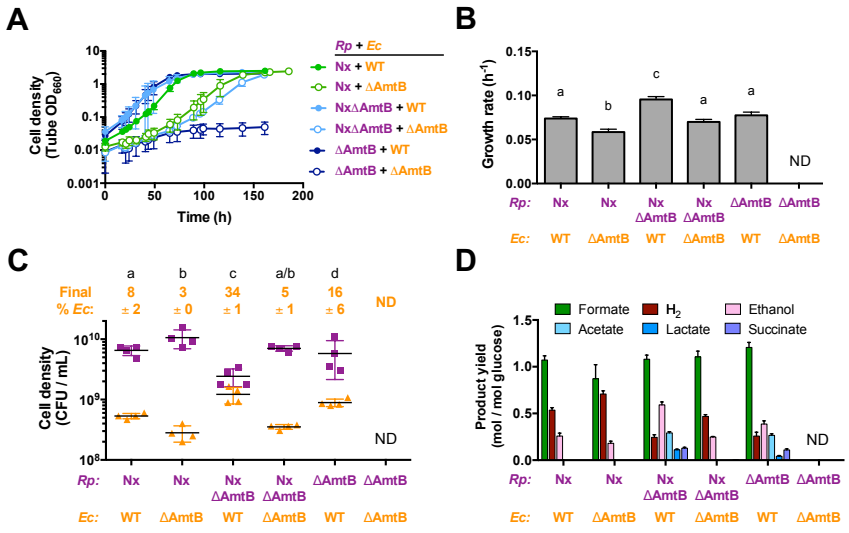


**Fig. 4. $NH_4^+$ transporters influence population and metabolic trends of both partners in coculture.** Growth curves (**A**), growth rates (**B**), final cell densities after one culturing (**C**), and fermentation product yields (**D**) from cocultures of all combinations of mutants lacking AmtB in each species. Final cell

479 densities and fermentation product yields were taken after one week, within 24 h into stationary phase.
480 ND, not determined. Error bars indicate SD, n=4. Different letters indicate statistical differences, $p < 0.05$, determined by one-way ANOVA with Tukey's multiple comparisons post test.

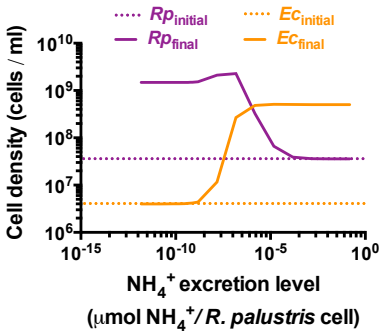


482

483 **Fig. 5. Higher *R. palustris* $NH_4^+$ excretion levels are predicted to compensate for a low *E. coli* $NH_4^+$**
484 **affinity.** 300 h batch cultures were simulated with a relative *R. palustris* : *E. coli* (*Ec* : *Rp*) $K_m$ value for
485 $NH_4^+$ of 0.001 over different *R. palustris* $NH_4^+$ excretion levels ($R_A$). Final cell densities, solid lines;
486 initial cell densities, dotted lines.

487

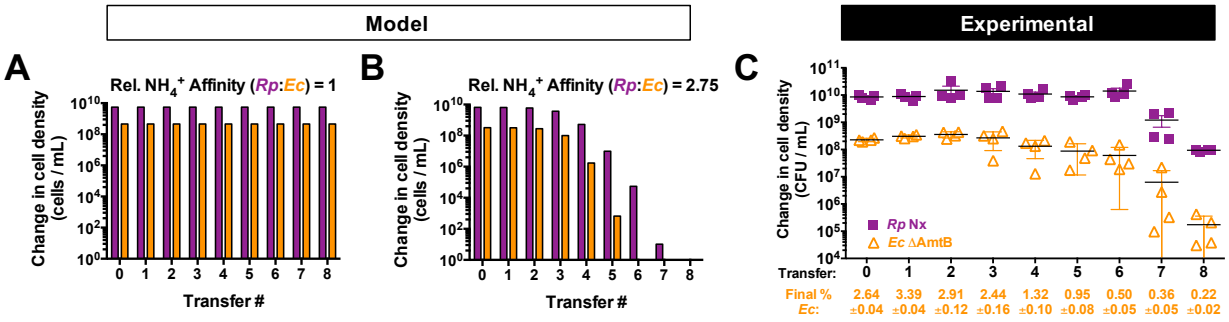


488

489 **Fig. 6. A low *E. coli* $NH_4^+$ affinity results in coculture collapse over serial transfers when paired**
490 **with *R. palustris* Nx.** (**A**,**B**) 300 h batch cultures were simulated and serial transferred used a 1%
491 inoculum based on the cell density at 300 h for the previous culture. Relative $NH_4^+$ affinity values
492 represent the relative *E. coli* $K_m$ for $NH_4^+$ ($K_A$) divided by that of *R. palustris* ($K_{AR}$). (**C**) Final cell
493 densities of *R. palustris* Nx and *E. coli* ΔAmtB of cocultures grown for one week, less than 24 h into
494 stationary phase. A 1% inoculum was used for each subsequent serial transfer. Error bars indicate SD,
495 n=4. Final *E. coli* cell percentages +/- SD for each transfer are shown.

# Recipient-biased competition for a cross-fed nutrient is required for coexistence of microbial mutualists

Alexandra L. McCully, Breah LaSarre, James B. McKinlay

Department of Biology, Indiana University, Bloomington

## SI Appendix.

### SyFFoN_v3 description.

Equations 1 – 4 were used to describe *E. coli* and *R. palustris* growth rates:

Eq. 1: *E. coli* growth rate; $\boldsymbol{\mu_{Ec}} = \mu_{EcMAX}\bullet[G/(K_G+G)]\bullet[A/(K_A+A)]\bullet[b_{Ec}/(b_{Ec}+10^{(f+C)})]$

Eq. 2: *R. palustris* growth rate ($N_2$); $\boldsymbol{\mu_{Rpn}} = \mu_{RpMAX}\bullet[C/(K_C+C)]\bullet[N/(K_N+N)]\bullet[b_{Rp}/(b_{Rp}+10^{(f+C)})]$

Eq. 3: *R. palustris* growth rate ($NH_4^+$); $\boldsymbol{\mu_{Rpa}} = \mu_{RpMAX2}\bullet[C/(K_C+C)]\bullet[A/(K_{AR}+A)]\bullet[b_{Rp}/(b_{Rp}+10^{(f+C)})]$

Eq 4: Total *R. palustris* growth rate; $\boldsymbol{\mu_{Rp}} = \mu_{Rpn}+ \mu_{Rpa}$

Equations 5-14 were used to describe temporal changes in cell densities and extracellular compounds. Numerical constants in product excretion equations are used to account for molar stoichiometric conversions. Numerical constants used in sigmoidal functions are based on those values that resulted in simulations resembling empirical trends. All R and r parameters are expressed in terms of glucose consumed except for $R_A$, which is the amount of $NH_4^+$ produced per *R. palustris* cell (Table S1).

Eq. 5: Glucose; $\boldsymbol{dG/dt} = -\mu_{Ec}\bullet Ec/Y_G - \mu_{Ec}\bullet Ec\bullet(R_c+R_f+R_e+R_{CO2}) - Ec\bullet(G/(K_G+G))\bullet(10/(10+1.09^{(1000\bullet\mu Ec)}))\bullet(b_{Ec}/(b_{Ec}+10^{(f+C)}))\bullet((100/(100+6^C))\bullet(r_C+r_f+r_e+r_{CO2}) + r_{C_mono} + r_{f_mono} + r_{e_mono} + r_{CO2_mono})$

Eq. 6: $N_2$; $\boldsymbol{dN/dt} = -\mu_{Rp}\bullet Rp\bullet 0.5\bullet Ra\bullet(1-(40/(40+1.29^N)) - \mu_{Rp}\bullet Rp/Y_N$

Eq. 7: Consumable organic acids; $\boldsymbol{dC/dt} = Ec\bullet\mu_{Ec}\bullet R_c\bullet 2 + Ec\bullet 2\bullet(G/(K_G+G))\bullet(10/(10+1.09^{(1000\bullet\mu Ec)}))\bullet(b_{Ec}/(b_{Ec}+10^{(f+C)}))\bullet(r_C\bullet(100/(100+6^C))+r_{C_mono}) - (\mu_{Rp}\bullet Rp/Y_C) - 0.25\bullet Rp\bullet\mu_{Rp}\bullet Rh_{Rp} - 0.25\bullet Rp\bullet r_{Hp}\bullet(C/(K_C+C))\bullet(40/(40+1.29^N))\bullet(b_{Rp}/(b_{Rp}+10^{(f+C)}))$

Eq. 8: Formate; $\boldsymbol{df/dt} = (Ec\bullet\mu_{Ec}\bullet R_f\bullet 6) + Ec\bullet 6\bullet(G/(K_G+G))\bullet(10/(10+1.09^{(1000\bullet\mu Ec)}))\bullet(b_{Ec}/(b_{Ec}+10^{(f+C)}))\bullet(r_f\bullet(100/(100+6^C)) + r_{f_mono}$

Eq. 9: $NH_4^+$; $\boldsymbol{dA/dt} = Rp\bullet\mu_{Rp}\bullet R_A\bullet(1-(40/(40+1.29^N))) - \mu_{Ec}\bullet Ec/Y_A - (\mu_{Rp}\bullet Rp/Y_{AR})\bullet(A/(K_{AR}+A))$

Eq. 10: *E. coli*; $\boldsymbol{dEc/dt} = \mu_{Ec}\bullet Ec$

Eq. 11: *R. palustris*; $\boldsymbol{dRp/dt} = \mu_{Rp}\bullet Rp$

Eq. 12: Ethanol; $\boldsymbol{de/dt} = Ec\bullet 3\bullet(\mu_{Ec}\bullet R_e + (G/(K_G+G))\bullet(10/(10+1.09^{(1000\bullet\mu Ec)}))\bullet(b_{Ec}/(b_{Ec}+10^{(f+C)}))\bullet(r_e\bullet(100/(100+6^C)) + r_{e_mono}))$

Eq. 13: $CO_2$; $\boldsymbol{dCO2/dt} = Ec \bullet 6 \bullet (\mu_{Ec} \bullet R_{CO2} + (G/(K_G+G)) \bullet (10/(10+1.09^{(1000 \bullet \mu Ec)})) \bullet (b_{Ec}/(b_{Ec}+10^{(f+C)})) \bullet (r_{co2} \bullet (100/(100+6^{C})) + r_{co2_mono})) + Rp \bullet 0.5 \bullet (\mu_{Rp} \bullet Rh_{Rp} + r_{Hp} \bullet (C/(K_C+C)) \bullet (40/(40+1.29^{N})) \bullet (b_{Rp}/(b_{Rp}+10^{(f+C)})))$

Eq. 14: $H_2$; $\boldsymbol{dH/dt} = Rp \bullet (\mu_{Rp} \bullet R_{HRp} + r_{Hp} \bullet (C/(K_C+C)) \bullet (40/(40+1.29^{N})) \bullet (b_{Rp}/(b_{Rp}+10^{(f+C)}))) + Ec \bullet (\mu_{Ec} \bullet R_{HEc} + (G/(K_G+G)) \bullet (10/(10+1.09^{(1000 \bullet \mu Ec)})) \bullet (b_{Ec}/(b_{Ec}+10^{(f+C)})) \bullet (r_H \bullet (100/(100+6^{C})) + r_{H_mono}))$

Where,

$\mu$ is the specific growth rate of the indicated species ($h^{-1}$).

$\mu_{MAX}$ is the maximum specific growth rate of the indicated species ($h^{-1}$).

G, A, C, N, f, e, H and CO2 are the concentrations (mM) of glucose, $NH_4^+$, consumable organic acids, $N_2$, formate, ethanol, $H_2$, and $CO_2$, respectively. All gasses are assumed to be fully dissolved. Consumable organic acids are those that *R. palustris* can consume, namely, lactate (3 carbons), acetate (2 carbons), and succinate (4 carbons). All consumable organic acids were simulated to have three carbons for convenience. Only net accumulation of formate, ethanol, $CO_2$ and $H_2$ are described in accordance with observed trends.

K is the half saturation constant for the indicated substrate (mM).

Ec and Rp are the cell densities (cells/ml) of *E. coli* and *R. palustris*, respectively.

b is the ability of a species to resist the inhibiting effects of acid (mM).

Y is the *E. coli* or *R. palustris* cell yield from the indicated substrate (cells / µmol glucose). Y values were determined in MDC with the indicated substrate as the limiting nutrient.

R is the fraction of glucose converted into the indicated compound per *E. coli* cell during growth (µmol of glucose / *E. coli* cell), except for $R_A$. Values were adjusted to accurately simulate product yields measured in cocultures and in MDC with and without added $NH_4Cl$.

$R_A$ is the ratio of $NH_4^+$ produced per *R. palustris* cell during growth (µmol / *R. palustris* cell). The default value was based on that which accurately simulated empirical trends.
r is the growth-independent rate of glucose converted into the indicated compound (µmol / cell / h). Default values are based on those which accurately simulated empirical trends in coculture.

$r_{_mono}$ is the growth-independent rate of glucose converted into the indicated compound by *E. coli* when consumable organic acids accumulate. Default values are based on linear regression of products accumulated over time in nitrogen-free cell suspensions of *E. coli* (4).

**Table S1. Default parameter values used in the model unless stated otherwise**

| Parameter | Value | Description (Units); Source |
|---|---|---|
| $\mu_{EcMAX}$ | 0.2800 | *E. coli* max growth rate ($h^{-1}$); Monoculture |
| $\mu_{RpMAX}$ | 0.0772 | *R. palustris* max growth rate ($h^{-1}$); Monoculture |
| $\mu_{RpMAX2}$ | 0.0152 | Boost on *R. palustris* growth rate in presence of $NH_4^+$ ($h^{-1}$); Monoculture[a] |
| G | 25 | Glucose (mM) |
| A | 0.00005 | $NH_4^+$ (mM); from initial $(NH_4)_6Mo_7O_{24}\cdot 4H_2O$ concentration |
| C | 0 | Consumable organic acids (those that *R. palustris* was observed to consume: lactate, acetate, and succinate; mM) |
| N | 70 | $N_2$ (assumed to be fully dissolved; mM) |
| f | 0 | Formate (mM) |
| e | 0 | Ethanol (mM) |
| CO2 | 0 | Carbon dioxide (mM) |
| $K_G$ | 0.02 | *E. coli* affinity (Michaelis-Menten constant ($K_m$)) for glucose (mM); (1) |
| $K_C$ | 0.01 | *R. palustris* affinity ($K_m$) for consumable organic acids (mM); Assumed |
| $K_A$ | 0.01 | *E. coli* affinity for $NH_4^+$ (mM); (2) |
| $K_{AR}$ | 0.01 | *R. palustris* affinity for $NH_4^+$ (mM); Assumed[b] |
| $K_N$ | 6 | *R. palustris* affinity ($K_m$) for $N_2$ (mM) |
| Ec | $0.4 \times 10^7$ | *E. coli* cell density (cells / ml) |
| Rp | $3.6 \times 10^7$ | *R. palustris* cell density (cells / ml) |
| $b_{Ec}$ | $10^{43}$ | Resistance of *E. coli* to low pH (mM) |
| $b_{Rp}$ | $10^{32}$ | Resistance of *R. palustris* to low pH (mM) |
| $Y_G$ | $8 \times 10^7$ | Glucose-limited *E. coli* growth yield (cells / µmol glucose); Glucose-limited *E. coli* culture |
| $Y_A$ | $1 \times 10^9$ | $NH_4^+$-limited *E. coli* growth yield (cells / µmol $NH_4^+$); $NH_4^+$-limited *E. coli* culture |
| $Y_C$ | $2.5 \times 10^8$ | Organic acid-limited *R. palustris* growth yield (cells / µmol organic acid); Acetate-limited *R. palustris* culture |
| $Y_N$ | $5 \times 10^8$ | $N_2$-limited *R. palustris* growth yield cells / µmol $N_2$; $N_2$-limited *R. palustris* culture |
| $R_C$ | $1.9 \times 10^{-8}$ | Fraction of glucose converted to organic acids (µmol glucose / cell) |
| $R_f$ | $8 \times 10^{-9}$ | Fraction of glucose converted to formate (µmol glucose / cell) |
| $R_e$ | $4.5 \times 10^{-9}$ | Fraction of glucose converted to ethanol (µmol glucose / cell) |
| $R_{CO2}$ | $5 \times 10^{-10}$ | Fraction of glucose converted to $CO_2$ (µmol glucose / cell) |
| $R_{HRp}$ | $2 \times 10^{-9}$ | *R. palustris* $H_2$ production (µmol $H_2$ / *R. palustris* cell) |
| $R_{HEc}$ | $5 \times 10^{-9}$ | *E. coli* $H_2$ production (µmol $H_2$ / *E. coli* cell) |
| $R_A$ | $0.15 \times 10^{-9}$ | *R. palustris* $NH_4^+$ production (µmol $NH_4^+$ / cell) |
| $r_C$ | $300 \times 10^{-11}$ | *E. coli* specific growth-independent rate of glucose conversion to consumable organic acids (µmol glucose / cell / h) (3) |
| $r_f$ | $47 \times 10^{-11}$ | *E. coli* specific growth-independent rate of glucose conversion to formate (µmol glucose / cell / h) (3) |
| $r_e$ | $15 \times 10^{-11}$ | *E. coli* specific growth-independent rate of glucose conversion to ethanol (µmol glucose / cell / h) (3) |
| $r_{CO2}$ | $2 \times 10^{-11}$ | *E. coli* specific growth-independent rate of glucose conversion to $CO_2$ (µmol glucose / cell / h) (3) |

| | | |
|---|---|---|
| $r_H$ | $2 \times 10^{-11}$ | *E. coli* specific growth-independent rate of $H_2$ production (μmol $H_2$ / cell / h) (3) |
| $r_{C_mono}$ | $1.2 \times 10^{-11}$ | *E. coli* specific growth-independent rate of glucose conversion to consumable organic acids when consumable organic acids accumulate (μmol glucose / cell / h); (4) |
| $r_{f_mono}$ | $0.83 \times 10^{-11}$ | *E. coli* specific growth-independent rate of glucose conversion to formate when consumable organic acids accumulate (μmol glucose / cell / h); (4) |
| $r_{e_mono}$ | $0.5 \times 10^{-11}$ | *E. coli* specific growth-independent rate of glucose conversion to ethanol when consumable organic acids accumulate (μmol glucose / cell / h); (4) |
| $r_{co2_mono}$ | $1.3 \times 10^{-11}$ | *E. coli* specific growth-independent rate of glucose conversion to $CO_2$ when consumable organic acids accumulate (μmol glucose / cell / h); (4) |
| $r_{H_mono}$ | $0.83 \times 10^{-11}$ | *E. coli* specific growth-independent rate of glucose conversion to $H_2$ when consumable organic acids accumulate (μmol glucose / cell / h); (4) |
| $r_{Hp}$ | $27 \times 10^{-11}$ | *R. palustris* specific growth-independent rate of $H_2$ production (μmol $H_2$ / cell / h) |

[a] Increased growth rate in presence of $NH_4^+$ versus $N_2$ based on the difference in experimentally determined growth rates in *R. palustris* monocultures grown with either $NH_4^+$ or $N_2$ as a nitrogen source.

[b] $K_{AR}$ was assumed to be equivalent to the published *E. coli* $K_m$ (2) for $NH_4^+$ ($K_A$).

91 **Table S2. Strains, plasmids, and primers used in this study**

| **Strain or plasmid** | **Description or Sequence (5'-3'); Designation** | **Source or Purpose** |
|---|---|---|
| ***R. palustris* strains** | | |
| CGA009 | Wild-type strain; spontaneous $Cm^R$ derivative of CGA001 | (5) |
| CGA4004 | CGA009 Δ*hupS* Δ*rpa2750*; Parent | (4) |
| CGA4005 | CGA4004 *nifA**; Nx | (4) |
| CGA4021 | CGA4005 Δ*amtB1* Δ*amtB2*; NxΔAmtB | (4) |
| CGA4026 | CGA4004 Δ*amtB1* Δ*amtB2;* ΔAmtB | This study |
| ***E. coli* strains** | | |
| MG1655 | Wild-type K12 strain, WT | (6) |
| K-12 JW0441-1 | Keio collection Δ*amtB::Km* | (7) |
| MG1655ΔAmtB | MG1655 Δ*amtB::Km*; ΔAmtB | This study |
| **Plasmids** | | |
| pJQnifA16 | $Gm^R$; WT *nifA* gene flanked by XbaI/BamHI cloned into pJQ200SK | This study |
| **Primers** | | |
| ALM6f | TTCGTCGCTGAATTGCAACG | *amtB* upstream flanking region (*E. coli*) |
| ALM6r | TCAGGAAGGGGTGATGCGTA | *amtB* downstream flanking region (*E. coli*) |
| JBM1 | CGTCTAGACCGGCGCATCGC | *nifA16* upstream primer; XbaI |
| JBM6 | GGGGATCCTGGTTCGCAGAGG | *nifA16* downstream primer; BamHI |

92

93 **SI Appendix Figures.**

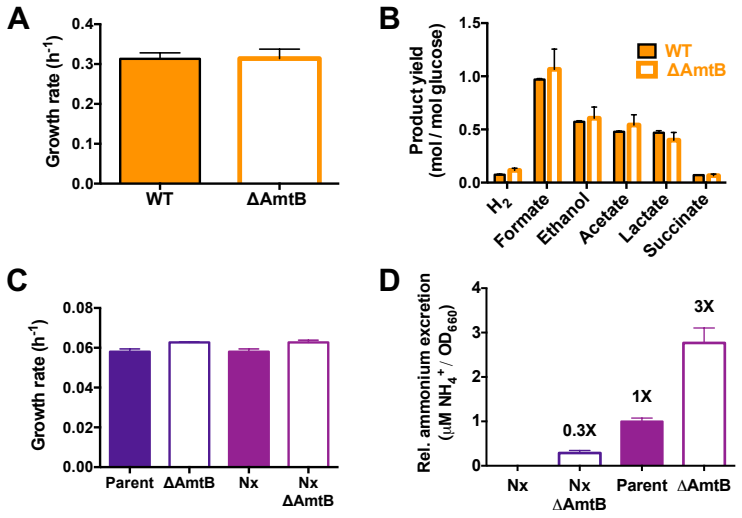


94

95 **Fig. S1. *E. coli* ΔAmtB and *R. palustris* ΔAmtB monoculture growth and metabolic trends.** (**A**,**B**)
96 Growth rates (**A**) and fermentation product yields (**B**) from WT *E. coli* (filled) or without (open) *E. coli*
97 ΔAmtB monocultures grown in MDC with 25 mM glucose and 15 mM $NH_4Cl$. Fermentation profiles were
98 generated from stationary monocultures. Error bars indicate SD, n=3. (**C**,**D**) Growth curves (**C**) and relative
99 $NH_4^+$ excretion (**D**) of *R. palustris* monocultures grown in MDC with 3 mM sodium acetate and a 100% $N_2$
100 headspace. Error bars indicate SD, n=4.

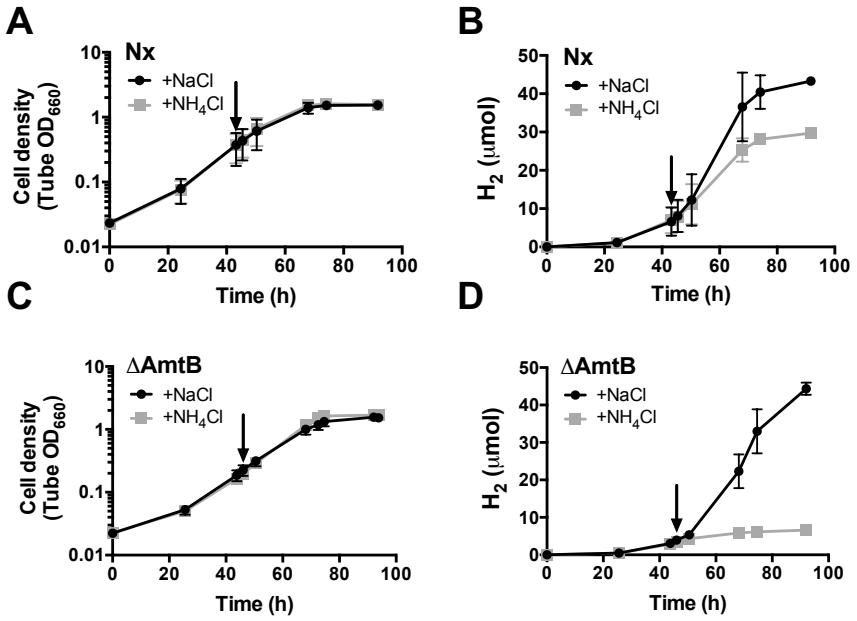


**Fig. S2. *R. palustris* ΔAmtB responds to $NH_4^+$-induced shutoff of nitrogenase.** The effect of either $NH_4Cl$ or NaCl on growth (**A**,**C**) and $H_2$ production (**B**,**D**) in *R. palustris* Nx or *R. palustris* ΔAmtB monocultures. *R. palustris* monocultures were grown in MDC with 20 mM sodium acetate and a 100% $N_2$ headspace until mid-exponential phase and then supplemented with either 15 mM $NH_4Cl$ or 15 mM NaCl at the time indicated by the arrow.

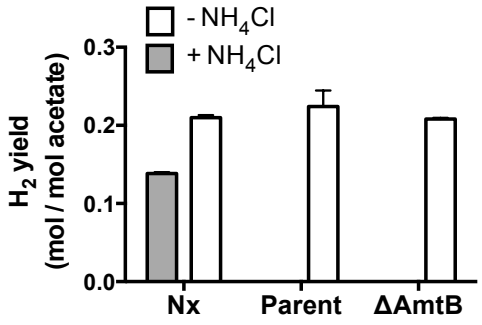


**Fig. S3. Unlike *R. palustris* Nx, *R. palustris* ΔAmtB does not produce $H_2$ when grown with $NH_4^+$.** *R. palustris* monocultures were grown in MDC with 20 mM sodium acetate and a 100% $N_2$ headspace with (grey) or without (white) 15mM $NH_4Cl$. Samples for determining $H_2$ yields were taken one week after inoculation, within 24 hours into stationary phase. Error bars indicate SD, n=3.

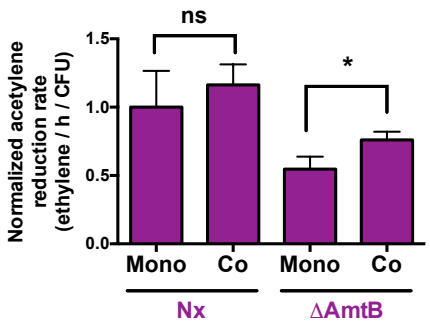


**Fig. S4. *R. palustris* ΔAmtB nitrogenase activity increases in coculture.** Normalized nitrogenase activity of *R. palustris* in monoculture (Mono) or coculture (Co) measured by an acetylene reduction assay. Ethylene levels were divided by total *R. palustris* CFUs in the test tube and then normalized to the *R. palustris* Nx monoculture value. Error bars indicate SD, n=4. *, statistical difference between monoculture and coculture conditions, $p < 0.05$, determined using multiple two-tailed t-tests; ns, no significant difference.

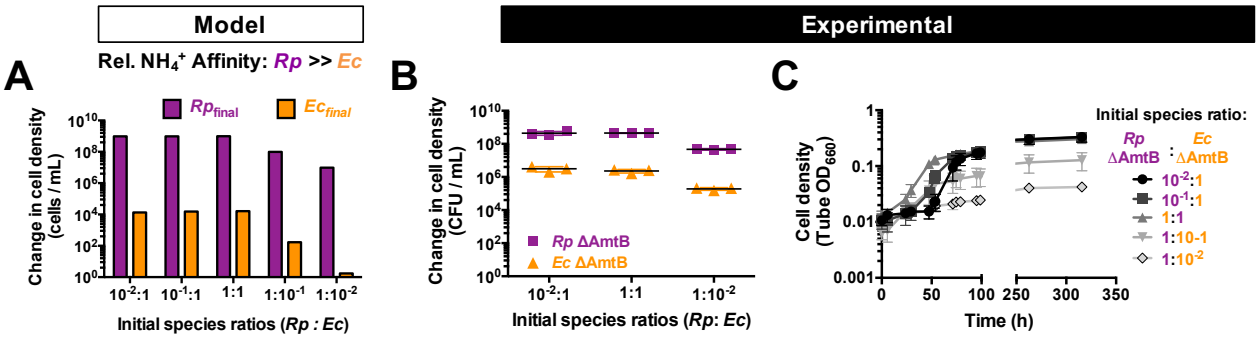


**Fig. S5. Higher initial cell densities of *E. coli* ΔAmtB can partially compensate for a low *E. coli* $NH_4^+$ affinity.** Simulations (**A**) and empirical data (**B**,**C**) showing the effect of initial *E. coli* (*Ec*) cell density on population and coculture growth trends when *E. coli* has a lower affinity for $NH_4^+$ compared to *R. palustris* (*Rp*). (**A**) 300 h batch cultures were simulated with a relative *R. palustris* : *E. coli* (*Rp* : *Ec*) $K_m$ value for $NH_4^+$ of 0.001. (**B, C**) Change in cell densities after one week of growth (**B**) and growth curves (**C**) of cocultures inoculated at different species ratios. (**A-C**) A ratio value of 1 represents 2.7 x $10^6$ CFUs/mL, which was experimentally measured from the starting inoculum for both species before diluting to achieve the indicated ratios. Error bars indicate SD, n=3.

130 **SI Appendix References.**


131 1. Buhr A, Daniels GA, Erni B. (1992) The glucose transporter of *Escherichia coli*: Mutants with impaired
132 translocation activity that retain phosphorylation activity. *J Biol Chem.* **267**(6):3847–3851.
133 2. Khademi S, et al. (2004) Mechanism of ammonia transport by Amt/MEP/Rh: structure of AmtB at 1.35 A.
134 *Science.* **305**(5690):1587–1594.
135 3. McCully AL, LaSarre B, McKinlay JB. (2017) Growth-independent cross-feeding modifies boundaries for
136 coexistence in a bacterial mutualism. *biorXiv*. **doi:** https://doi.org/10.1101/083386
137 4. LaSarre B, McCully AL, Lennon JT, McKinlay JB. (2017) Microbial mutualism dynamics governed by
138 dose-dependent toxicity of cross-fed nutrients. *ISME J*. **11**:337–348.
139 5. Larimer FW, et al. (2004) Complete genome sequence of the metabolically versatile photosynthetic bacterium
140 *Rhodopseudomonas palustris*. *Nat Biotechnol.* **22**(1):55–61.
141 6. Hayashi K, et al. (2006) Highly accurate genome sequences of *Escherichia coli* K-12 strains MG1655 and
142 W3110. *Mol Syst Biol.* **2**(1):2006.0007.
143 7. Baba T, et al. (2006) Construction of *Escherichia coli* K-12 in-frame, single-gene knockout mutants: the
144 Keio collection. *Mol Syst Biol.* **2**:2006.0008.